Charge Correlations in Ferromagnetic CMR Manganites

Raymond Osborn, Chairman

Neutron and x-ray evidence of charge melting in ferromagnetic layered colossal magnetoresistance manganites (invited)

L. Vasiliu-Doloc[a)]
Department of Physics, Northern Illinois University, DeKalb, Illinois 60115 and Advanced Photon Source, Argonne National Laboratory, Argonne, Illinois 60439

R. Osborn, S. Rosenkranz, J. Mesot,[b)] and J. F. Mitchell
Materials Science Division, Argonne National Laboratory, Argonne, Illinois 60439

S. K. Sinha and O. H. Seeck[c)]
Advanced Photon Source, Argonne National Laboratory, Argonne, Illinois 60439

J. W. Lynn
NIST Center for Neutron Research, National Institute of Standards and Technology, Gaithersburg, Maryland 20899

Z. Islam
Department of Physics, Northern Illinois University, DeKalb, Illinois 60115 and Advanced Photon Source, Argonne National Laboratory, Argonne, Illinois 60439

Recent x-ray and neutron scattering studies have revealed static diffuse scattering due to polarons in the paramagnetic phase of the colossal magnetoresistive manganites $La_{2-2x}Sr_{1+2x}Mn_2O_7$, with $x = 0.40$ and 0.44. We show that the polarons exhibit short-range incommensurate correlations that grow with decreasing temperature, but disappear abruptly at the combined ferromagnetic and metal–insulator transition in the $x = 0.40$ system because of the sudden charge delocalization, while persisting at low temperature in the antiferromagnetic $x = 0.44$ system. The ''melting'' of the polaron ordering as we cool through T_C occurs with the collapse of the polaron scattering itself in the $x = 0.40$ system. This short-range polaron order is characterized by an ordering wave vector $q = (0.3, 0, 1)$ that is almost independent of x for $x \geq 0.38$, and is consistent with a model of disordered stripes. © *2001 American Institute of Physics.* [DOI: 10.1063/1.1365256]

INTRODUCTION

Doped manganese oxides have attracted tremendous interest both because they exhibit anomalously large magnetoresistance effects near the Curie temperature, and because the physics of this class of materials is related to the high-T_c superconducting copper oxides. Like the cuprates, these materials are in the vicinity of an insulator–metal transition, as well as magnetic and structural instabilities, but they do not become superconducting. They exhibit other exotic properties instead, such as colossal magnetoresistance (CMR)—a dramatic increase in the conductivity when the system orders ferromagnetically, either by cooling or by applying a magnetic field. The basic relationship between ferromagnetism and conductivity has been understood in terms of the double-exchange mechanism,[1] where an itinerant e_g electron hops between Mn^{+4} ions, providing both the ferromagnetic exchange and electrical conduction. In addition, these systems are characterized by an unusually strong coupling among spin, charge, and lattice degrees of freedom, which can be tuned by varying the electronic doping, electronic bandwidth, and disorder. Therefore, an understanding of these materials must include, in addition to the double-exchange mechanism and strong electron correlations, a strong electron–phonon interaction.[2]

The two-layer Ruddlesden–Popper compounds $La_{2-2x}Sr_{1+2x}Mn_2O_7$,[3] where x is the nominal hole concentration, are derived from the perovskite structure of the three-dimensional cubic compounds $La_{1-x}A_xMnO_3$ (A=Sr, Ca, Ba) by interleaving the network of corner-shared MnO_6 octahedra with nonmagnetic (La,Sr)O blocking layers. This reduces the dimensionality of the system and strongly enhances the spin and charge fluctuations. The crystal structure is body-centered tetragonal (space group $I4/mmm$)[4] with $a \simeq 3.87$ Å and $c \simeq 20.15$ Å. In the intermediate doping regime ($0.32 \leq x < 0.42$), the ground state is a ferromagnetic metal, and the magnetoresistance is found to be strongly enhanced near the combined metal–insulator and Curie transition at T_C (112 K for the $x = 0.40$ system of present interest[5]).

[a)]Electronic mail: doloc@physics.niu.edu
[b)]Present address: Laboratory for Neutron Scattering, ETH-Zürich and Paul Scherrer Institut, CH-5232 Villigen-PSI, Switzerland.
[c)]Present address: Forschungszentrum Jülich, IFF 8, 52425 Jülich, Germany.

The measurements described here were performed on two single crystals of the double-layer compound: one with $x=0.40$, $La_{1.2}Sr_{1.8}Mn_2O_7$, with dimensions $6\times4\times1$ mm³, cleaved from a boule that was grown using the floating-zone technique,[4] and a second one with $x=0.44$, $La_{1.12}Sr_{1.88}Mn_2O_7$, cylindrical in shape with an average radius of 5 mm and 2 cm long, also grown using the floating-zone technique in the Materials Science Division at Argonne. The x-ray data were taken on the 1-ID-C diffractometer at the Advanced Photon Source, mostly using a high-energy beam of 36 keV to provide enough penetration in transmission geometry. Additional measurements were taken in reflection geometry with 21 keV. The neutron measurements were performed on the BT-2 triple-axis spectrometer at the NIST Center for Neutron Research, using both unpolarized (with either energy integration or energy analysis) and polarized neutron beams with an incident energy of 13.7 meV. For the measurements under magnetic field at BT-2, we employed a superconducting solenoid to provide fields up to 9 T applied in the ab plane. A wide range of reciprocal space was explored, including the $(h0l)$ and (hhl) planes.

THE $x=0.40$ SYSTEM

The existence of polarons in the paramagnetic phase of the CMR systems has been invoked theoretically in order to explain the behavior of the resistivity with temperature, and has been inferred from a variety of measurements.[6] However, direct observation via diffuse x-ray or neutron scattering in single crystals had been lacking. A polaron consists of a localized charge with its associated lattice distortion field which gives rise to diffuse scattering around the Bragg peaks, known as Huang scattering. Recent x-ray measurements have revealed anisotropic diffuse scattering centered on Bragg peaks in the paramagnetic phase of the optimally doped $x=0.40$ bilayer compound $La_{1.2}Sr_{1.8}Mn_2O_7$.[7] Figure 1(a) shows a contour plot of the diffuse x-ray scattering in the $(h0l)$ plane around the (200) Bragg reflection.[8] Because of its particular symmetry, this diffuse scattering has been called "butterfly" scattering. The butterfly scattering has a strong temperature dependence, with a dramatic response at T_C, as illustrated in Fig. 1(b) which shows a series of x-ray h scans through the diffuse scattering in Fig. 1(a) that reveal two symmetric lobes of scattering. Figure 1(c) shows the temperature dependence of the intensity of these two lobes. The almost linear temperature dependence of the diffuse scattering below T_C in Fig. 1(c) suggests that phonons dominate in this temperature regime,[9] but the abrupt change at T_C is not due to conventional phonons. This was confirmed by neutron energy scans, which revealed both quasielastic and inelastic (phonon) contributions.[7] The phonon contribution is well separated from the quasielastic scattering and was found to obey the usual Bose thermal population factor, whereas the quasielastic intensity increases with decreasing temperature, but then collapses below T_C. This demonstrates that the change at T_C in the (energy integrated) x-ray diffuse scattering is entirely due to the quasielastic contribution, showing that the lattice distortions giving rise to it are quasistatic on a time scale $\tau\sim1$ ps set by the energy resolution of the instru-
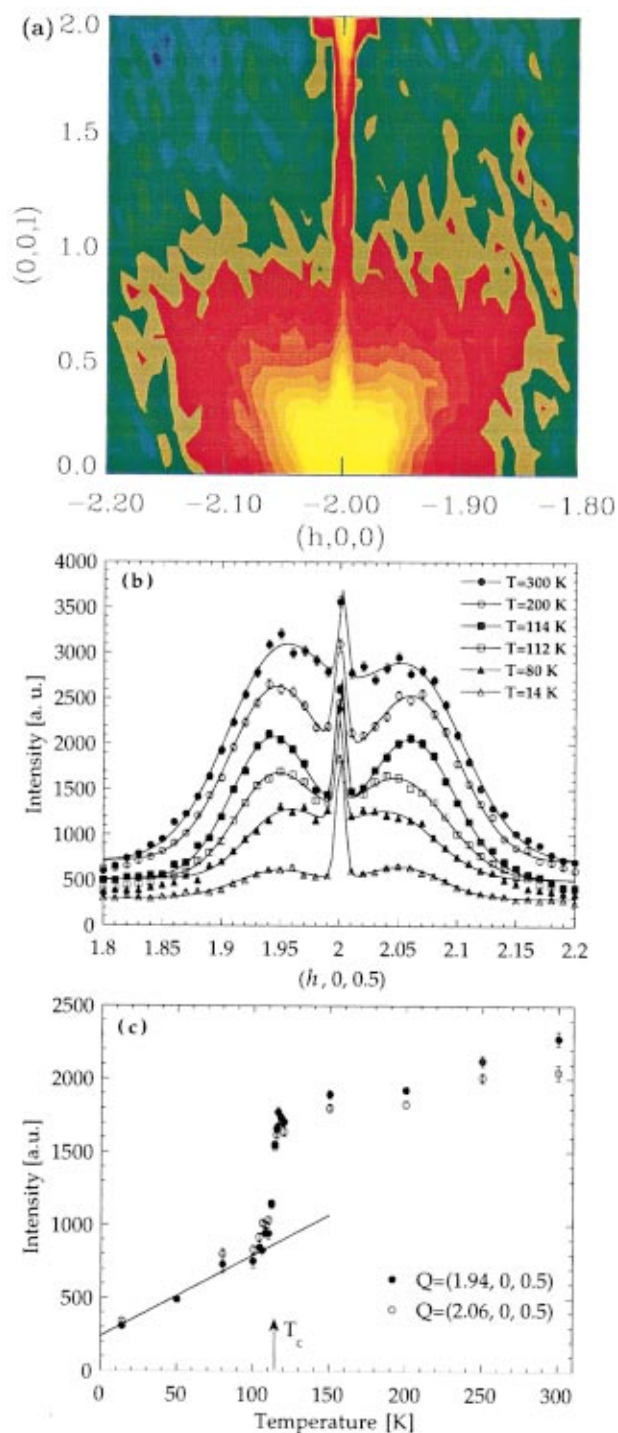

FIG. 1. (Color) (a) Contour plot showing the lobe-shaped pattern of diffuse x-ray scattering at $T=300$ K around the (200) reflection in the $x=0.40$ system. (b) X-ray h scans across the diffuse scattering around (200) at $l=0.5$ at a series of temperatures. The solid curves are fits to Gaussian functions. (c) Observed temperature dependence of the two $l>0$ lobes of x-ray diffuse scattering around (200). The straight line at low T is the estimated phonon contribution (thermal diffuse scattering), while the jump near T_C is due to the formation of polarons.

ment (i.e., they are static on the time scale of typical phonon vibrations[7]). A good description of the **q** dependence of the butterfly scattering was obtained in terms of Huang scattering, consistent with a Jahn–Teller type distortion around the Mn^{3+} ions. Indeed, the localization of an e_g electron on a
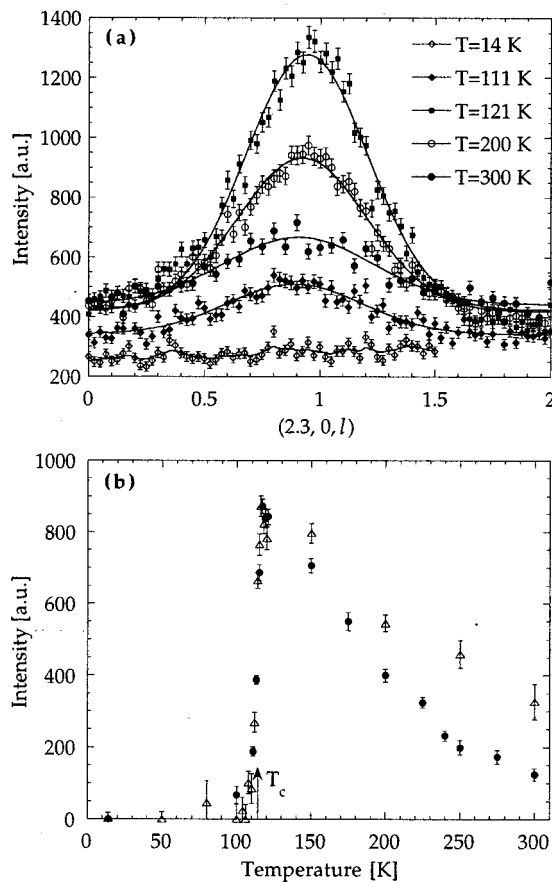
FIG. 2. (a) X-ray l scans through the satellite peak (2.3, 0, 1) at different temperatures. The solid curves are fits to Lorentzian functions. (b) Temperature dependence of the intensity of the (2.3, 0, 1) peak (closed circles) and of the x-ray diffuse scattering after correction for the phonon contribution (open triangles).

Mn site distorts the MnO_6 octahedron, which perturbs the surrounding lattice, and this strain field extends over several unit cells. The diffuse (butterfly) scattering centered on Bragg peaks results from the long-range strain field thus created. Similar diffuse scattering patterns have been observed in perovskite manganites.[10,11] Our results link directly the diffuse scattering to the existence of quasistatic polarons above T_C that disappear abruptly upon cooling below the ferromagnetic transition, where the charges delocalize in this CMR system.

In addition, these polarons are correlated at short range, as revealed by the presence of broad satellite peaks in the paramagnetic phase. These peaks are characterized by a wave vector $(\pm\epsilon, 0, \pm 1)$ as measured from the nearest fundamental Bragg peak, where $\epsilon \simeq 0.3$ [in terms of reciprocal lattice units $(2\pi/a, 0, 2\pi/c)$]. Figure 2(a) shows x-ray l scans through the incommensurate peak position (2.3, 0, l) at different temperatures. As is evident from Fig. 2(b), the intensity of this peak increases and then rapidly decreases in intensity as we cool through T_C. Neutron energy scans at the peak positions have shown that the correlations giving rise to these peaks are once again quasistatic on a time scale $\tau \sim 1$ ps, similar to the polaron (butterfly) scattering. Polarized neutron measurements performed to probe the nature of this scattering have shown that these peaks have no magnetic

component, but are purely structural. Thus the incommensurate satellite peaks originate most likely from Mn^{3+}–Mn^{4+} charge/orbital correlations that are incommensurate with the crystal lattice. One strong argument in favor of this interpretation is the abrupt disappearance of the intensity of the satellite peaks [closed circles in Fig. 2(b)] upon cooling below the ferromagnetic and coincident insulator-to-metal transition, where the charges delocalize. From Fig. 2(b) we can also see that the temperature dependence of the satellite peak intensity is remarkably similar to the Huang scattering (open triangles) derived from the x-ray diffuse scattering by subtracting the estimated thermal diffuse scattering [straight line in Fig. 1(c)]. This indicates that both types of scattering are associated with the development of polarons above T_C. The Huang (butterfly) scattering is due to individual polarons, while the incommensurate peaks are due to polaron correlations, which become stronger with decreasing temperature. Below T_C we observe a ''melting'' of the polaron correlations occurring simultaneously with the collapse of the polarons themselves.

The superlattice peaks are broader than the q resolution in both h and l directions, showing that the in-plane and out-of-plane charge correlations remain relatively short range at all temperatures. Correlation lengths estimated from the q widths are weakly temperature dependent, and peak at the same temperature as the intensity, with ~ 26.4 Å $\sim 6a$ in plane, and ~ 10.4 Å $\sim c/2$ out of plane [see Fig. 3(a)]. The correlation length in the transverse k direction is about two times shorter than in the longitudinal h direction. No higher harmonics have been observed, and no $(\pm\epsilon, \pm\epsilon, \pm 1)$ superlattice peaks have been found. The short-range nature of the polaron correlations makes it difficult to perform quantitative comparisons to polaron ordering models. Nevertheless, we made such an attempt and collected more than 100 satellite reflections and identified the atomic displacements involved. The results of this comprehensive analysis will be published elsewhere.[12] Here we will only draw some qualitative conclusions from the (hkl) dependence of the superlattice peaks concerning the lattice displacements that produce them. They indicate that Jahn–Teller distortions of the Mn^{3+} ions line up in stripes parallel to the Mn–O–Mn bonds. Since the superlattice peaks occur close to the commensurate positions $\epsilon = \frac{1}{3}$, Fig. 3(b) provides an idealized picture of the closest commensurate charge/orbital ordering. The closed circles indicate Mn^{3+} sites, with the e_g $3x^2 - r^2$ ($3y^2 - r^2$) orbitals oriented in the (a,b) plane, producing displacements of the oxygen atoms at the corners of the corresponding MnO_6 octahedra along the a (b) axis. We cannot infer from our data the precise charge/orbital configuration between these stripes, so the open circles indicate both Mn^{4+} sites and some Mn^{3+} sites with the e_g orbitals oriented perpendicular to the modulation direction. The ''orbital'' stripes, as they may be called because of the orbital ordering involved in this picture, are stacked on top of each other in the two MnO_2 planes within a bilayer. However, the $l =$ odd integer component of the ordering wave vector, which is related to the presence of two MnO_2 bilayers per unit cell, indicates that distortions produced by the modulation of the charge density are, on average, out of phase in adjacent bilayers. The small
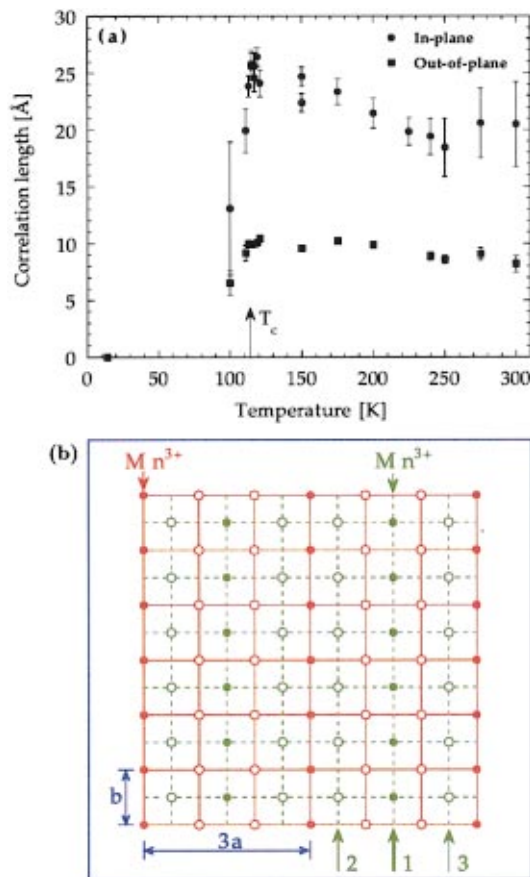
FIG. 3. (Color) (a) In-plane and out-of-plane correlation lengths estimated from the satellite peak q widths. (b) Possible charge-ordering pattern for the closest commensurate configuration $\epsilon = 1/3$. Closed circles denote Mn^{3+} sites, and open circles denote a mixture of Mn^{3+} with e_g orbitals oriented out of plane and Mn^{4+} sites. The solid and dotted lines are the square lattices of Mn atoms in adjacent bilayers. The arrows indicate the possible positions of the Mn^{3+} stripe in the adjacent bilayer: 1 ($p_1 \sim 1/2$) is the most likely position due to Coulomb repulsion or lattice strain, while there is a reduced probability ($p_2 = p_3 \sim 1/4$) that the stripe occurs on either side of the preferred location.
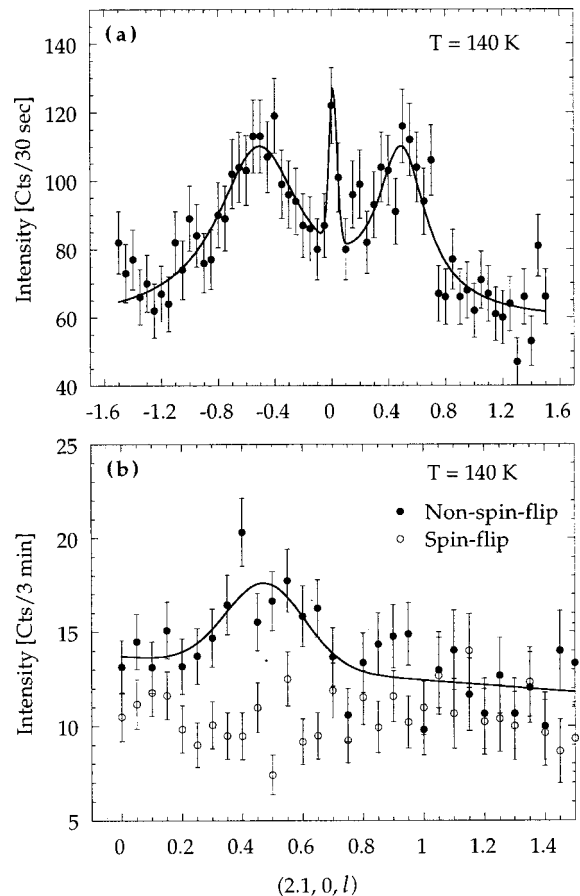
FIG. 4. (a) Neutron l scan across the diffuse scattering around (200) at $h = 2.1$ and $T = 140$ K in the $x = 0.44$ system, showing two symmetric lobes of scattering. (b) l scan across one of the lobes measured with polarized neutrons: nonspin-flip scattering (closed circles) and spin-flip scattering (open circles).

c-axis correlation length ($\simeq$ the separation between two bilayers) suggests that only two bilayers are correlated at most, and in view of the large separation between bilayers, the Hendricks–Teller model[13] can be used in which stripes in adjacent bilayers are statistically arranged according to a simple probabilistic model. The solid and dotted lines in Fig. 3(b) denote the square lattices of manganese atoms in one MnO_2 bilayer (red) and in an adjacent bilayer (green), respectively. The arrows indicate the possible positions of the Mn^{3+} stripes in the adjacent bilayer: 1 is the most likely position due to Coulomb repulsion or overlapping strain fields, while there is a reduced probability that the stripe occurs on either side of the preferred location. By assigning a probability $p_1 = 1/2$ to out-of-phase position 1, and a probability $p_2 = p_3 = 1/4$ to positions 2 and 3, we have calculated the scattering and found that it produces Lorentzian-like peaks at odd l, with tails extending to the nearest even l's, as observed experimentally [see Fig. 2(a)].

Although the picture in Fig. 3(b) seems similar to the charge stripes that have been observed in the insulating and antiferromagnetically ordered cubic manganites,[14] as well as the superconducting cuprates and nickelates,[15,16] there are important differences. First, in the cubic manganites, the charge stripes are oriented 45° away from the Mn–O–Mn bonds. In the present compound, the absence of (ϵ, ϵ, l) reflections indicates that the charge stripes must be oriented along the Mn–O–Mn bonds. Second, the short correlation lengths, particularly in the transverse direction, indicate that the system breaks up into short orbital stripe fragments that are highly disordered in the transverse direction.

THE $x = 0.44$ SYSTEM

The $x = 0.44$ bilayer system $La_{1.12}Sr_{1.88}Mn_2O_7$ no longer has a metallic ferromagnetic ground state, in contrast to the $x = 0.40$ system. It has a Néel transition at $T_N \simeq 136$ K and a spin canting transition at $T_C \simeq 87$ K corresponding to the onset of a ferromagnetic moment, whose low temperature value is an order of magnitude smaller than the antiferromagnetic moment. The anisotropic butterfly scattering is present in this system as well, as indicated by the neutron l scan at $T = 140$ K displayed in Fig. 4(a), showing two lobes of diffuse scattering[17] on one side of the (200) Bragg reflection. Polarized neutron measurements have indicated that this diffuse scattering is purely structural. Figure 4(b) shows an l scan across one of the lobes in Fig. 4(a) performed with
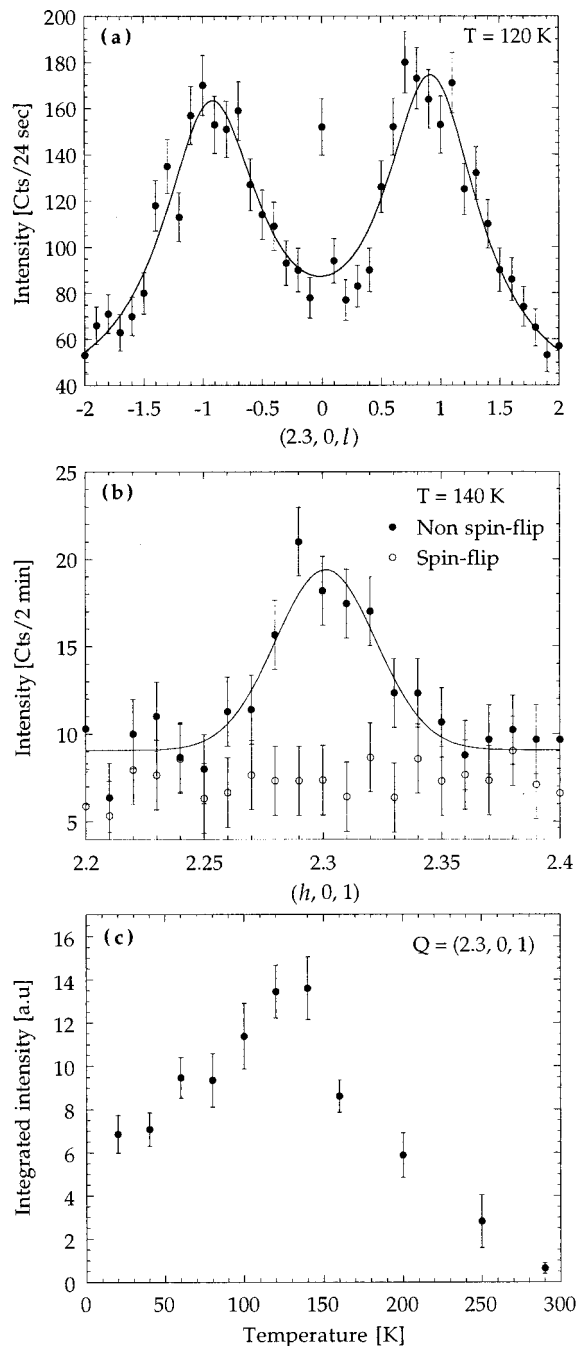
FIG. 5. (a) Neutron l scan through the charge-ordering peaks at $(2.3, 0, \pm 1)$ at $T = 120$ K. (b) h scan through the satellite peak $(2.3, 0, 1)$ measured with polarized neutrons: nonspin-flip scattering (open circles) and spin-flip scattering (closed circles). (c) Temperature dependence of the $(2.3, 0, 1)$ satellite peak in the $x = 0.44$ system.

polarized neutrons. In the configuration where the neutron polarization $\mathbf{P} \parallel \mathbf{Q}$ (the neutron wave vector), we found that all the scattering was nonspin flip [closed circles in Fig. 4(b)], while any magnetic scattering would be spin flip [open circles in Fig. 4(b)]. Therefore, similar to the $x = 0.40$ system, the presence of polarons gives rise to Huang scattering centered on Bragg peaks. Moreover, the polarons are correlated at short range with the same ordering wave vector $(0.3, 0, 1)$, as in the $x = 0.40$ system. Figure 5(a) shows a neutron scan along the l direction through the incommensurate peak positions $(2.3, 0, l)$, revealing two broad symmetric peaks at $l = \pm 1$. Figure 5(b) shows a scan along the h direction through the $(2.3, 0, 1)$ peak performed at $T = 140$ K with polarized neutrons, indicating that the incommensurate peaks are purely structural reflections in this system as well. It thus seems that the short-range polaron ordering characterized by the ordering wave vector $(0.3, 0, 1)$ is very robust. We have observed it in the more lightly doped $x = 0.38$ system. Recently, it has also been seen in the $x = 0.45$ and 0.48 systems.[18] In this wide concentration range, $0.38 \leq x \leq 0.48$, the ordering wave vector is approximately the same, and thus seems to be almost independent of the doping level. This feature is puzzling and is yet to be explained. Figure 5(c) shows the temperature dependence of the $(2.3, 0, 1)$ satellite peak. Above T_N, the polaron correlations become stronger with decreasing temperature. At T_N the intensity starts decreasing, but it never disappears completely, persisting at low temperatures. This behavior was expected, and correlates very well with the behavior of the resistivity versus T, because the $x = 0.44$ system does not have a metallic ferromagnetic ground state.

DISCUSSION

Charge and orbital ordering have been observed in a number of insulating, antiferromagnetic cubic manganites,[14,19,20] as well as in layered manganites with $x = 0.5$.[21] However, charge ordering is incompatible with double-exchange mediated ferromagnetism seen in optimally doped CMR systems. Therefore, the short-range charge correlations observed in the paramagnetic phase of the $x = 0.40$ bilayer compound represent a novel feature. The charge correlations result from Coulomb interactions between the polarons, coupled with the interaction of overlapping elastic strain fields. Since our measurements, such short-range charge correlations have been observed in a number of perovskite manganites, although with a different ordering wave vector,[22,23] and may be a universal feature of ferromagnetic CMR compounds.

In the $x = 0.40$ system these charge correlations are not strong enough to win the competition with the double-exchange interaction, and the charges delocalize at the ferromagnetic transition, where the polaron correlations melt and the lattice strain relaxes. On the other hand, in the $x = 0.44$ system the double exchange is not strong enough to induce a three-dimensional (3D) ferromagnetic transition. In this system it is the charge correlations that win the competition with the double-exchange interaction, and the charges remain localized at low temperature in the canted antiferromagnetic structure. It is the delicate balance among double exchange, Coulomb repulsion, and the orbitally induced lattice strain fields that dictates whether the material is a ferromagnetic metal or charge-ordered insulator at low temperatures.

ACKNOWLEDGMENTS

[1] C. Zener, Phys. Rev. **82**, 403 (1951); J. B. Goodenough, *ibid.* **100**, 564 (1955).

[2] See, for example, A. J. Millis, P. B. Littlewood, and B. I. Shraiman, Phys. Rev. Lett. **74**, 5144 (1995); H. Röder, J. Zang, and A. R. Bishop, *ibid.* **76**, 1356 (1996); A. J. Millis, Phys. Rev. B **53**, 8434 (1996); A. S. Alexandrov and A. M. Bratkovsky, Phys. Rev. Lett. **82**, 141 (1999).

[3] Y. Moritomo, A. Asamitsu, H. Kuwahara, and Y. Tokura, Nature (London) **380**, 141 (1996).

[4] J. F. Mitchell, D. N. Argyriou, J. D. Jorgensen, D. G. Hinks, C. D. Potter, and S. D. Bader, Phys. Rev. B **55**, 63 (1997).

[5] R. Osborn, S. Rosenkranz, D. N. Argyriou, L. Vasiliu-Doloc, J. W. Lynn, S. K. Sinha, J. F. Mitchell, K. E. Gray, and S. D. Bader, Phys. Rev. Lett. **81**, 3964 (1998).

[6] S. J. L. Billinge, R. G. DiFrancesco, G. H. Kwei, J. J. Neumeier, and J. D. Thompson, Phys. Rev. Lett. **77**, 715 (1996); D. Louca, T. Egami, E. L. Brosha, H. Röder, and A. R. Bishop, Phys. Rev. B **56**, R8475 (1997).

[7] L. Vasiliu-Doloc *et al.*, Phys. Rev. Lett. **83**, 4393 (1999).

[8] The sharp rod of scattering along the $[0, 0, l]$ direction is resolution limited in the $(hk0)$ plane, and is associated with stacking faults inevitably found in crystals with layered structures.

[9] Such diffuse scattering patterns have also been seen in doped lanthanum nickelates and cuprates, but with a conventional temperature dependence; see, for example, E. D. Isaacs, G. Aeppli, P. Zschack, S.-W. Cheong, H. Williams, and D. J. Buttrey, Phys. Rev. Lett. **72**, 3421 (1994).

[10] S. Shimomura, N. Wakabayashi, H. Kuwahara, and Y. Tokura, Phys. Rev. Lett. **83**, 4389 (1999).

[11] S. Shimomura, T. Tonegawa, K. Takima, N. Wakabayashi, N. Ikeda, T. Shobu, Y. Noda, Y. Tomioka, and Y. Tokura, Phys. Rev. B **62**, 3875 (2000).

[12] B. J. Campbell *et al.* (unpublished).

[13] S. Hendricks and E. Teller, J. Chem. Phys. **10**, 147 (1942).

[14] S. Mori, C. H. Chen, and S.-W. Cheong, Nature (London) **392**, 473 (1998); S. Mori, C. H. Chen, and S.-W. Cheong, Phys. Rev. Lett. **81**, 3972 (1998).

[15] J. M. Tranquada, B. J. Sternlieb, J. D. Axe, Y. Nakamura, and S. Uchida, Nature (London) **375**, 561 (1995); J. M. Tranquada, J. D. Axe, N. Ichikawa, Y. Nakamura, S. Uchida, and B. Nachumi, Phys. Rev. B **54**, 7489 (1996).

[16] C. H. Chen, S.-W. Cheong, and A. S. Cooper, Phys. Rev. Lett. **71**, 2461 (1993).

[17] The central peak may indicate a different symmetry of the butterfly scattering. We are currently conducting investigations to look into the possible origins of this central peak.

[18] M. Kubota, Y. Oohara, H. Yoshizawa, H. Fujioka, K. Shimizu, K. Hirota, Y. Moritomo, and Y. Endoh, J. Phys. Soc. Jpn. **69**, 1986 (2000).

[19] Y. Murakami *et al.*, Phys. Rev. Lett. **81**, 582 (1998).

[20] Y. Endoh *et al.*, Phys. Rev. Lett. **82**, 4328 (1999).

[21] J. Q. Li, Y. Matsui, T. Kimura, and Y. Tokura, Phys. Rev. B **57**, R3205 (1998).

[22] C. P. Adams, J. W. Lynn, Y. M. Mukovskii, A. A. Arsenov, and D. A. Shulyatev, Phys. Rev. Lett. **85**, 3954 (2000).

[23] P. Dai, J. A. Fernandez-Baca, N. Wakabayashi, E. W. Plummer, Y. Tomioka, and Y. Tokura, Phys. Rev. Lett. **85**, 2553 (2000).